

RELATIVISTIC STERN-GERLACH DEFLECTION

Richard Talman, Laboratory for Elementary-Particle Physics, Cornell University

ABSTRACT

Modern advances in polarized beam control should make it possible to accurately measure Stern-Gerlach (S-G) deflection of relativistic beams. Toward this end a relativistically covariant S-G formalism is developed that respects the opposite behavior under inversion of electric and magnetic fields. Not at all radical, or even new, this introduces a distinction between electric and magnetic fields that is not otherwise present in pure Maxwell theory. Experimental configurations (mainly using polarized electron beams passing through magnetic or electric quadrupoles) are described. Electron beam preparation and experimental methods needed to detect the extremely small deflections are discussed.

INTRODUCTION

Our purpose is to produce a relativistically-valid (though not quantum mechanical) theory of the deflection of a particle, such as an electron (or more practically, a beam of electrons), in a non-uniform electromagnetic magnetic field. We refer to such deflection as “Stern-Gerlach (S-G) deflection”, but without intending to imply that quantum-mechanical effects, such as the splitting of quantized states, can be enabled.

We also neglect spin precession. This will limit the applicability of the formulation to the passage through magnets short enough for spin precession (calculable by the BMT equation) to be negligible. Furthermore, for simplicity, we initially consider only on-axis passage through a quadrupole magnet. As it happens, since the magnetic field on the quadrupole axis vanishes, in this case there will be neither electromagnetic deflection nor spin precession. But there will be S-G deflection, leading to (still negligible) electromagnetic effects in subsequent approximation.

Physical constants to be used in this paper for electron charge and electron magnetic moment are

$$\begin{aligned} e &= 1.60217662 \times 10^{-19} \text{ C}, \\ e_e^* &= -e, \\ \mu_B &= \frac{e\hbar}{2m_e} = 5.7883818066 \times 10^{-5} \text{ eV/T}, \\ \mu_e^* &= (2.00231930436182/2) \mu_B. \end{aligned} \quad (1)$$

These values are given to such exaggerated accuracy only to emphasize that they are experimentally-measured and well known. However a copying error on one of these values, say in the fifth decimal place, would have no practical effect whatsoever on the experimentally challenging deflections predicted in this paper (because they are so small).

Furthermore there will be no discussion of subtleties such as anomalous magnetic moments.

For reference, the fine structure constant and the speed of light are given by

$$\begin{aligned} \alpha &= \frac{e^2}{4\pi\epsilon_0\hbar c} = \frac{1}{137.03600}, \\ c &= 2.99792458 \times 10^8 \text{ m/s}. \end{aligned} \quad (2)$$

One slightly off-key note in constants (1) may be noticeable; e_e^* and μ_e^* have asterisks attached, suggesting that, under some circumstances, for example in different frames of reference, their values might be different. For the case of e_e we know that charge is a true scalar and that this will never happen, so introducing the symbol e_e^* is pure pedantry; following tradition, the asterisk will therefore be dropped for electric charge. But, multiplying a vector, the magnetic moment μ_e^* is more subtle, and examples of μ_e depending on reference frame exist in the literature. Following Conte[1] the asterisk on μ_e^* will be adopted. The interpretation of the asterisk (which, for consistency, would also be attached to charge e) is that μ_e^* must never have any value other than that given in Eqs. (1).

Other off-key steps will also be taken, the most troubling of which may be the (temporary) divorce of electric and magnetic fields. Deviating from Coulomb, it was Faraday who visualized electric field lines emerging from point charges. This made it natural, for example to Poisson, to visualize magnetic field lines emerging from north or south magnetic poles. But Oersted and Ampère made it more natural to treat currents as the sources of magnetic field. And Maxwell made it all but axiomatic to treat electric and magnetic fields as so married as to be inseparable. Here (for purely pedagogical purposes) we take the (temporary) retrograde step of divorcing electric and magnetic fields (while being careful not to contradict well understood phenomena).

Just as it is electric field \mathbf{E} that applies a force to a charge e at rest, it will be (non-uniform) magnetic field \mathbf{B} that applies a force to magnetic moment μ_e^* at rest. In this paper we consider only electric and magnetic fields that are transverse to particle motion. (With just one peripheral exception) we consider only (almost) straight line motion along a “longitudinal” axis. Lorentz boosts occur only along this axis, and fields that are transverse in any frame are transverse in every frame. The vector operator ∇ can therefore, if one wishes, be everywhere replaced by ∇_\perp . (This would not be valid at entrances and exits of magnets or electric elements, but we are neglecting such end effects, if necessary assuming they cancel in pairs.) Other than time-variation associated with entering or exiting deflection elements, all

fields are assumed to be time-independent.

Expressed as equations, we take, as *defining* relations for rest frame electric and Stern-Gerlach forces,

$$\mathbf{F}^{\text{elec}} = -e\mathbf{E}, \quad (3)$$

$$\begin{aligned} \mathbf{F}^{SG} &= \frac{\mu_e^*}{c} (\hat{\mathbf{s}}^* \cdot \nabla) c\mathbf{B} \\ &= \mu_e^* \nabla (\hat{\mathbf{s}}^* \cdot \mathbf{B}). \end{aligned} \quad (4)$$

Here, $\hat{\mathbf{s}}^*$ is a unit spatial 3-vector specifying the orientation of the spin angular momentum in the rest frame. Only short elements, for which $\hat{\mathbf{s}}^*$ can be treated as constant, will be considered. In this case, since $\nabla \times \mathbf{B} = 0$, it is valid to move $\hat{\mathbf{s}}^*$ inside the ∇ operator in the second of Eqs. (4). This has promoted magnetic moment (over magnetic charge) to rank with electric charge as the partners of magnetic and electric fields respectively. Factors of c introduced, then cancelled, in Eq. (4) are an artifact of MKS units, the result of E and cB having the same units. To the extent that it is “natural” for the magnitudes of E and cB to be comparable, the ratio of Stern-Gerlach to electromagnetic force is determined by a ratio of coupling constants:

$$\frac{\mu_B/c}{e} = 1.930796 \times 10^{-13} \text{ m}, \quad (5)$$

where, except for anomalous magnetic moment and sign, Bohr magneton μ_B is the electron magnetic moment. This ratio has the dimension of length, compensating the inverse length coming from the spatial derivative in Eq. (4).

BRIEF HISTORICAL PERSPECTIVE

It seems fair to say that the role played by the Stern-Gerlach force in the development of quantum mechanics has been almost as important as electric field has been in the development of electromagnetic theory. It is curious, then, that Eq. (3) has been confirmed to accuracy approaching that implied by physical constants (1), while Eq. (4) has never been confirmed to much better than the 10 percent or so accuracy of the original Stern-Gerlach experiment[2][3].

The poor quality (even after a century) of experimental checks of Stern-Gerlach deflection can probably be ascribed to the smallness of ratio (5). The present paper is motivated partly by the desire to improve this experimental determination. Since such a check is likely to use a particle storage ring, it is essential to generalize Eq. (4) to moving particles, especially having speed v approaching the speed of light c .

It might be thought that these generalizations are already well known and uncontroversial. Certainly, the relativistic version of Eq. (3) is well known, initially by Maxwell, later by Einstein, and thoroughly described, for example by Jackson[4]. Furthermore the precession of the spin vector itself, in relativistic motion, has been predicted by Thomas and by Bargmann, Michel, and Telegdi (BMT) and confirmed experimentally.

However the Stern-Gerlach deflection of relativistic electrons, as well as being controversial theoretically, has

never been observed experimentally. That is, the influence of a particle’s spin orientation (whose evolution is assumed known) on a relativistic particle’s orbit is not well understood. The orbit influence is known, however, to be so small that a further iteration to describe any resulting perturbation of the spin orientation would be gratuitous.

This paper is concerned with just this single aspect of the Stern-Gerlach phenomenon; namely spin-dependent particle deflection, to be referred to here as Stern-Gerlach (S-G) particle deflection. Unlike the original S-G experiment, this does not need any quantum-mechanical separation of spin states in the uniform magnetic field component of an applied magnetic field. Rather it is assumed that a polarized beam, prepared upstream, passes on-axis through a quadrupole representing the non-uniform magnetic field that causes S-G deflection.

There exists a Bohr-Pauli “theorem” (or at least argument) proving the impossibility of replicating the original Stern-Gerlach experiment with electrons. The argument is clearly explained by Mott and Massey[5], especially in their Figure 36. The argument combines the inevitable transverse beam sizes implied by the Heisenberg uncertainty principle (for a beam with finite energy spread) with the extreme weakness of the on-axis S-G bending relative to off-axis electromagnetic bending. In modern accelerator jargon, even with the beam height being minimized by a beam waist at the deflection point, rotation of the phase space beam ellipse downstream of a quadrupole overwhelms the S-G beam shift of any single particle relative to the full beam height.

Itself always controversial, this Bohr argument, in any case, applies to the deflection of single electrons, for their eventual downstream separation. It does not apply directly to the downstream centroid shift of a beam that has been pre-polarized upstream of the S-G deflecting magnet. Nowadays, with beam centroid shifts small compared to beam size being observed routinely (for example in Schottky detectors) this argument has become somewhat suspect.

It is argued here that modern storage ring developments have made it possible to measure the extremely small orbit centroid shifts caused by the S-G deflection of a pre-polarized beam of electrons, thereby making Eq. (4) more precise.

This is not intended to include any claim that an unpolarized electron beam can be split into two polarized electron beam by S-G deflection. And, in fact, it seems inevitable that any S-G orbit shift (presumably of order 1Å or less at most locations in a storage ring) will always be less than achievable electron beam sizes.

LORENTZ FORCE LAW

The relativistic generalization of electromagnetic force to moving particles requires another empirical law, the Lorentz force law, which is reviewed next, mainly to make the electromagnetic field tensor available:

$$\mathbf{F}^{\text{e.m.}} = -e(\mathbf{E} + e\mathbf{v} \times \mathbf{B}). \quad (6)$$

Table 1: The main 4-vectors to be used, as well as the 2-index, anti-symmetric electromagnetic 4-tensor \mathbb{F} . Font selection can be inferred from this table. Typically unprimed variables refer to a general frame of reference, such as the laboratory, and primed variables refer to a frame in which the particle is either at rest, or moving at non-relativistic velocity. Transverse spin vector \mathbf{s}_\perp and longitudinal spin component s_\parallel Lorentz transform differently, as given in Eq. (14).

symbol	definition	contravariant components	rest frame	name	invariant
X	X	(ct, \mathbf{r})	(ct', \mathbf{r}')	4-displacement	$c^2\tau^2$
U	$d\mathbf{X}/d\tau$	$(\gamma c, \gamma \mathbf{v})$	$(c, 0)$	4-velocity	c^2
P	$m_e \mathbf{U}$	$(E/c, \mathbf{p})$	$(mc, 0)$	4-energy-momentum	$m^2 c^2$
W	Eq. (10)	$(\mathbf{s} \cdot \mathbf{p}, (\mathcal{E}/c)\mathbf{s})$	$(0, m_e c \mathbf{s}')$	Pauli-Lubanski 4-spin	$-m^2 c^2$
S	$\mathbf{S} = \mathbf{W}/(mc)$	$(\gamma \mathbf{s} \cdot \boldsymbol{\beta}, \gamma \mathbf{s})$	$(0, \mathbf{s}')$	4-spin	$- \mathbf{s}' ^2$
\square		$(\partial/\partial(ct), \boldsymbol{\nabla})$	$(\partial/\partial(ct'), \boldsymbol{\nabla}')$	4-gradient	
\mathbb{F}		Eq. (7)		EM-field-tensor	

Following Jackson, and/or Steane[6], but skipping many details, we introduce contravariant (upper index) and covariant (lower index) tensors, shown (in various representations) in Table 1. 4D dot product invariants are defined as by Steane, except with reversed metric tensor signs. This dot product notation allows many subscripts and superscripts to be suppressed and the distinction between contravariant and covariant components to be largely hidden. An “electric” (as unconventionally contrasted here with “magnetic”) field tensor is defined by

$$\mathbb{F}(\mathbf{E}, \cdot) = \begin{pmatrix} 0 & E^1/c & E^2/c & E^3/c \\ -E^1/c & 0 & -B^3 & B^2 \\ -E^2/c & B^3 & 0 & -B^1 \\ -E^3/c & -B^2 & B^1 & 0 \end{pmatrix} \quad (7)$$

(Also unconventionally) this tensor is formally expressed here as a function $\mathbb{F}(\mathbf{E}, \cdot)$ of the electric field *vector*, irrespective of the fact that it depends also on the components of \mathbf{B} which, if present at all, are subsidiary and are represented only by a dot in the argument list.

This notation favors reference frames in which the magnetic field actually vanishes, since the only non-vanishing elements are in the first row (which influences energy changes) and the first column (which influences momentum changes). It will soon be clear that this notation is really just an insignificant, artificial way of guiding the discussion. Having said earlier, in connection with Eqs. (3) and (4), that \mathbf{E} and \mathbf{B} fields are not to be treated as components of the same “physical object”, it probably seems to be cheating to combine them, as in this equation. The B^i components in this equation will shortly be associated with the B^i components in Eq. (4) and it will be convenient then, not to have to change their symbols.

Eq. (7) also differs slightly from Jackson’s conventions in that the components are expressed with raised indices, in spite of the fact that there is no contravariant/distinction for 3D vector components, which are usually given lower indices. When matching 3D coordinates with 4D coordinates, while encouraging the use, by default, of contravariant indices for 4D fields and coordinates, it is less confusing to use upper indices for 3D components.

There is a more significant issue with definition (7). As

Fitzpatrick[8] explains, Eq. (7), as written, seems inconsistent with our understanding that \mathbf{B} is a pseudo-vector, while \mathbf{E} is a vector. Reflection or transition from right- to left-handed coordinate axes, would change the meaning of the equation. It might seem to be less inconsistent to express the magnetic components as $B^1 = B_{23}$, $B^2 = B_{31}$, $B^3 = B_{12}$, but this has, effectively, already been accomplished by shifting the positions of the magnetic components in the matrix. As long as one uses only coordinate frames not involving reflections, it is legitimate to mix vectors and pseudovectors in this way and, following convention, we tolerate this limitation.

Applying Eq. (7), Newton’s law for the Lorentz force law can be written in abbreviated form as

$$m_e \frac{d\mathbf{U}}{d\tau} = -e \mathbb{F}(\mathbf{E}, \cdot) \cdot \mathbf{U}. \quad (8)$$

Expressed (as matrix product) in the rest frame, this produces covariant acceleration components, expressed as a column matrix

$$\begin{pmatrix} dU^0/d\tau & -dU^{1'}/d\tau & -dU^{2'}/d\tau & -dU^{3'}/d\tau \end{pmatrix}^T = \frac{-e}{m_e} \begin{pmatrix} 0 & E^{1'}/c & E^{2'}/c & E^{3'}/c \\ -E^{1'}/c & 0 & -B^{3'} & B^{2'} \\ -E^{2'}/c & B^{3'} & 0 & -B^{1'} \\ -E^{3'}/c & -B^{2'} & B^{1'} & 0 \end{pmatrix} \begin{pmatrix} c \\ 0 \\ 0 \\ 0 \end{pmatrix}, \quad (9)$$

where the $B^{i'}$ components are ineffective not because they vanish, but because they multiply velocity components which do vanish. In this frame it seems legitimate to express \mathbb{F} as a function of only \mathbf{E} . In the laboratory frame $\mathbb{F}(\mathbf{E}, \cdot)$ is given by Eq. (7) and \mathbf{U} by $(\gamma c, \gamma \mathbf{v})^T$.

RELATIVISTIC STERN-GERLACH DEFLECTION

The least familiar entry in Table 1 is the Pauli-Lubanski spin tensor \mathbf{W} , which is a momentum-weighted spin vector defined by covariant components

$$\begin{aligned} W_a &= \frac{1}{2} \epsilon_{\lambda a \mu \nu} P^\lambda S^{\mu \nu} \\ &= \left((s_\parallel \hat{\boldsymbol{\beta}} + \mathbf{s}_\perp) \cdot \mathbf{p}, -(1/c) \mathcal{E} (s_\parallel \hat{\boldsymbol{\beta}} + \mathbf{s}_\perp) \right) \end{aligned} \quad (10)$$

where $\epsilon_{\lambda\alpha\mu\nu}$ is a standard 4-index tensor with non-vanishing components equal to ± 1 , depending on whether the indices are an even or odd permutation of 0,1,2,3, (and hence anti-symmetric in all indices), and $S^{\mu\nu}$ is a 2-index spin tensor.

Suppose that, relative to the rest frame, the laboratory frame is moving with velocity $-v\hat{\mathbf{x}}$. The inverse boost coordinate transformation giving (ct, \mathbf{x}) in terms of (ct', \mathbf{x}') is

$$\begin{aligned} ct &= \gamma(ct' + \boldsymbol{\beta} \cdot \mathbf{x}') \\ \mathbf{x} &= \mathbf{x}' + \left(-\gamma ct' + \frac{\gamma^2}{1+\gamma} \boldsymbol{\beta} \cdot \mathbf{x}' \right) \boldsymbol{\beta}. \end{aligned} \quad (11)$$

For \mathbf{W} to be a valid 4-vector requires it to be subject to the same Lorentz transformation. This requires the component expressions on the right hand side of Eq. (10) to be valid in all frames. To check that this is indeed the case, one can perform Lorentz boost (11) to 4-vector \mathbf{W}' to produce contravariant laboratory frame components

$$\begin{aligned} s_{\parallel} p &\stackrel{?}{=} \mathbf{W}^0 = \gamma \boldsymbol{\beta} \cdot m c \mathbf{s}' = \gamma m v s'_{\parallel} = s'_{\parallel} p, \\ (1/c) \mathcal{E} (s_{\parallel} \hat{\boldsymbol{\beta}} + \mathbf{s}_{\perp}) &\stackrel{?}{=} \\ \mathbf{W} &= m c \mathbf{s}' + \frac{\gamma^2}{1+\gamma} \beta^2 m c s'_{\parallel} \hat{\boldsymbol{\beta}} \\ &= m c (\mathbf{s}' - s'_{\parallel} \hat{\boldsymbol{\beta}}) + m c \left(1 + \frac{\gamma^2 \beta^2}{1+\gamma} \right) s'_{\parallel} \hat{\boldsymbol{\beta}} \\ &= (1/c) \mathcal{E}' \left(s'_{\parallel} \hat{\boldsymbol{\beta}} + \frac{\mathbf{s}'_{\perp}}{\gamma} \right). \end{aligned} \quad (12)$$

where the questioned equalities on the left can be answered in the affirmative if and only if the right hand side of Eq. (10) is valid in all reference frames. To make these formulas self-consistent, and to answer the questions in the affirmative requires

$$s_{\parallel} = s'_{\parallel}, \quad \text{and} \quad \mathbf{s}_{\perp} = \frac{\mathbf{s}'_{\perp}}{\gamma}. \quad (14)$$

These, therefore, are the Lorentz transformed components of spin 4-vector \mathbf{S} . (It is important to comment that these components will *not* appear in the relativistically-invariant Stern-Gerlach equation (26), whose derivation is our immediate goal.)

The spatial 3-vector \mathbf{s} has constant magnitude in any particular reference frame, and is the spatial part of the conventional (BMT) 4-spin vector. In the rest frame

$$\mathbf{W}' = m c \mathbf{S}' = (0, m c \mathbf{s}'). \quad (15)$$

The momentum weighting of the Pauli-Lubarski 4-vector is removed when \mathbf{W} is reduced to “helicity”

$$s_{\parallel} = \frac{\mathbf{s} \cdot \mathbf{p}}{p}. \quad (16)$$

A formula valid in one reference frame can be extended to other frames using what I will call the “Hagedorn Principle”, though the principle was undoubtedly introduced by

someone before him, probably Einstein. Here the principle is copied verbatim from Hagedorn (including the boxed format).

If an equation given in a particular Lorentz system can be written in a manifestly covariant form (that is, both sides have the same transformation property!) which in the particular Lorentz frame reduces to the equation given originally, this covariant form is the unique generalization of the equation given.

For invariant expression of the S-G deflection we need to follow the same path as was used for electromagnetic deflection, but with one change, brought out by the fact that the magnetic field is, in fact, a pseudo-vector. Jackson, in Eq. (11.140), defines a “dual”, 2-index, covariant tensor

$$\begin{aligned} \mathfrak{F}(\cdot, \mathbf{B}) &= \frac{1}{2} \epsilon_{\alpha\beta\gamma\delta} \mathbb{F}^{\gamma\delta} \\ &= \begin{pmatrix} 0 & B^1 & B^2 & B^3 \\ -B^1 & 0 & E^3/c & -E^2/c \\ -B^2 & -E^3/c & 0 & E^1/c \\ -B^3 & E^2/c & -E^1/c & 0 \end{pmatrix} \end{aligned} \quad (17)$$

It differs from \mathbb{F} by the replacements $\mathbf{E}/c \rightarrow \mathbf{B}$ and $\mathbf{B} \rightarrow -\mathbf{E}/c$. This time we have (artificially) expressed $\mathfrak{F}(\cdot, \mathbf{B})$ as a function only of \mathbf{B} as a reminder that it is appropriate for representing pseudo-vectors. This notation is most convenient for magnets at rest. Note that, even though E and B have different dimensions in MKS units, that “dual” tensors $\mathbb{F}(\mathbf{E})$ and $\mathfrak{F}(\cdot, \mathbf{B})$, in MKS units are both measured in Tesla magnetic field units.

With S-G force given by Eq. (4), copying from Eq. (8), but using $\mathfrak{F}(\cdot, \mathbf{B})$ because the argument is a pseudo-vector, we obtain

$$m_e \frac{d\mathbf{U}'}{d\tau} = \mu_e^* \mathfrak{F}(\cdot, (\mathbf{s}' \cdot \nabla') \mathbf{B}') \cdot \frac{\mathbf{U}'}{c}, \quad (18)$$

as the rest frame equation of motion. The final factor is divided by c because of MKS units. The Hagedorn principle can not yet be applied to this formula because the argument of \mathfrak{F} is expressed as a 3-vector rather than a 4-vector. Fortunately we are dealing with fields that are constant in time. This is violated only at particle entry and exit from the element causing the deflections. Even if there is a non-zero deflection on entry, it will be cancelled on exit. In the rest frame, where $\mathcal{E} = m c^2$ we can therefore make the replacement

$$\mathbf{s}' \cdot \nabla' = -\frac{\mathbf{W}'}{m c} \cdot \square' \quad (19)$$

where \square is defined in Table 1, to produce

$$m_e \frac{d\mathbf{U}'}{d\tau} = -\mu_e^* \mathfrak{F} \left(\cdot, \left(\frac{\mathbf{W}'}{m c} \cdot \square' \right) \mathbf{B}' \right) \cdot \frac{\mathbf{U}'}{c}. \quad (20)$$

This is now expressed in terms of invariant quantities.

Fortunately we do not need the full generality indicated by Eq. (20). We are interested in the perturbation, to a straight line on-axis orbit through a quadrupole, caused by

the S-G force. Let us say the axis in question carries the label “1”. (For standard accelerator coordinates “1” would naturally be replaced by “z”. But standard discussions of Lorentz boosts usually assume a particle is moving along the “x” axis in the laboratory, which is why we make this choice.) We are also restricting the generality by assuming that the longitudinal components of both \mathbf{E} and \mathbf{B} vanish in both the laboratory and rest frames.

For simplicity we can also treat purely transverse and purely longitudinal polarization separately. Let us start with just transverse polarization; i.e. replace \mathbf{s} by \mathbf{s}_\perp , meaning (for motion along the x^1 -axis) that $s_1 = 0$. With these specializations the rest frame equation of motion becomes

$$m_e \frac{dU'}{d\tau} = -\mu_e^* \mathfrak{F} \left(\cdot, \left(\frac{W'_\perp}{mc} \cdot \square'_\perp \right) \mathbf{B}'_\perp \right) \cdot \frac{\mathbf{U}'}{c}. \quad (21)$$

Under our assumed special conditions, the transverse (x^2, x^3) coordinates are conserved in the Lorentz transformation along the x^1 axis. These coordinates can therefore be treated as parameters, immune from alteration during boosts along the particle velocity axis. Also, because of the linearity of the matrix multiplication, the expression in large parentheses can be moved from argument to coefficient;

$$m_e \frac{dU'}{d\tau} = -\mu_e^* \left(\frac{W'_\perp}{mc} \cdot \square'_\perp \right) \mathfrak{F}(\cdot, \mathbf{B}'_\perp) \cdot \frac{\mathbf{U}'}{c}. \quad (22)$$

Applying the Hagedorn principle, the laboratory frame equation of motion is

$$m_e \frac{dU}{d\tau} = -\mu_e^* \left(\frac{W_\perp}{mc} \cdot \square_\perp \right) \mathfrak{F}(\cdot, \mathbf{B}_\perp) \cdot \frac{\mathbf{U}}{c}. \quad (23)$$

After these manipulations, Eq. (21) can more readily be compared with the electromagnetic force equation (8). In particular, $\mathfrak{F}(\cdot, \mathbf{B}_\perp) \cdot \mathbf{U}/c$ is relativistically invariant, like $\mathbb{F}(\mathbf{E}, \cdot) \cdot \mathbf{U}$. And the operations acting on $\mathfrak{F}(\mathbf{B}_\perp) \cdot \mathbf{U}/c$ in Eq. (21) preserve this frame invariance.

According to Eq. (14) rest frame transverse polarization is also transverse in the laboratory. And the azimuthal polarization angle is the same in rest frame and lab frame. Expressed in terms of the rest frame polarization vector \mathbf{s}'_\perp , the laboratory frame polarization vector is

$$\mathbf{s}_\perp = \frac{1}{\gamma} \mathbf{s}'_\perp = \frac{s_x'^2 \hat{\mathbf{x}}_2 + s_x'^3 \hat{\mathbf{x}}_3}{\gamma}. \quad (24)$$

The reason this replacement is appropriate is that the transverse magnetic moment vector is defined (only in the rest frame) to be $\mu_e^* \mathbf{s}'_\perp$. For substitution into laboratory equation of motion (21), and including longitudinal polarization

terms as well, we have

$$\begin{aligned} \frac{W_\perp}{m_e c} &= \left(0, \frac{\mathcal{E}}{m_e c^2} \frac{s_x'^2 \hat{\mathbf{x}}_2 + s_x'^3 \hat{\mathbf{x}}_3}{\gamma} \right) \\ &= (0, s_x'^2 \hat{\mathbf{x}}_2 + s_x'^3 \hat{\mathbf{x}}_3), \\ \square_\perp &= \left(0, \hat{\mathbf{x}}_2 \frac{\partial}{\partial x^2} + \hat{\mathbf{x}}_3 \frac{\partial}{\partial x^3} \right), \\ \frac{W_\parallel}{m_e c} &= \left(\gamma \frac{v}{c}, 0 \right), \quad \square_\parallel = (0, \hat{\mathbf{x}}_1 \partial / \partial x^1), \\ \frac{W}{m_e c} \cdot \square &= -s_x'^2 \frac{\partial}{\partial x^2} - s_x'^3 \frac{\partial}{\partial x^3} = -\hat{\mathbf{s}}^* \cdot \nabla_\perp. \end{aligned} \quad (25)$$

In the final step we have taken advantage of $W_\parallel \cdot \square_\parallel = 0$, and that all fields are independent of x^1 . Also we have re-introduced the same rest frame unit vector $\hat{\mathbf{s}}^*$ as appeared in Eq. (4). Its asterisk emphasizes that it is a unit vector in the rest frame, in spite of the fact that all other quantities in the equation of motion, including ∇_\perp , refer to the laboratory frame.

Finally, substituting from Eqs. (25) into Eq. (21), for transverse fields independent of time and longitudinal position, the frame-invariant Stern-Gerlach equation of motion is

$$m_e \frac{dU}{d\tau} = \mu_e^* \hat{\mathbf{s}}^* \cdot \mathfrak{F}(\cdot, \nabla \mathbf{B}) \cdot \frac{\mathbf{U}}{c}. \quad (26)$$

This formula is especially convenient in reference frames in which $\mathbf{E}=0$. As before, in reference frames where the electric field does not, in fact, vanish, the \cdot in the first argument has to be replaced by $\nabla \mathbf{E}$.

DEFLECTION EXAMPLES

Transverse fields (relative to the velocity \mathbf{v} , which we will take to be along the $\hat{\mathbf{x}}_1$ -axis) in the laboratory (unprimed) and in the electron rest frame (primed), are related by

$$\begin{aligned} \mathbf{E}' &= \gamma(\mathbf{E} + \mathbf{v} \times \mathbf{B}), \\ \mathbf{B}' &= \gamma(\mathbf{B} - \mathbf{v} \times \mathbf{E}/c^2). \end{aligned} \quad (27)$$

Expressed in terms of components,

$$\begin{aligned} E^{2'} &= \gamma(E^2 - vB^3), & E^{3'} &= \gamma(E^3 + vB^2), \\ B^{2'} &= \gamma(B^2 + vE^3/c^2), & B^{3'} &= \gamma(B^3 - vE^2/c^2). \end{aligned} \quad (28)$$

Particle Deflection in Electrostatic Separator

For practice with the covariant formulation, using entries from Table 1, we consider the deflection of an electron of velocity $v\hat{\mathbf{x}}_1$ in the transverse electric field $E\hat{\mathbf{x}}_2$ in a laboratory electrostatic separator of length L_E . Using $d/d\tau = \gamma d/dt$, Eq. (8), in laboratory coordinates, produces contravariant time derivative

$$-\frac{dp^2}{dt} = \frac{-e}{\gamma} \begin{pmatrix} 0 & 0 & E/c & 0 \\ 0 & 0 & 0 & 0 \\ -E/c & 0 & 0 & 0 \\ 0 & 0 & 0 & 0 \end{pmatrix} \begin{pmatrix} \gamma c \\ \gamma v \\ 0 \\ 0 \end{pmatrix} \Big|_2 = eE. \quad (29)$$

So the force is $dp^2/dt = -eE$, the duration L_E/v , the transverse impulse $-eEL_E/v$, and the angular deflection is

$$\Delta\theta_2 \approx \frac{-eEL_E/v}{p}, \quad (30)$$

which is the transverse momentum impulse divided by the longitudinal momentum.

As a check, the same result can be obtained by realizing the rest frame magnetic field, though non-zero, applies no force to a particle at rest; the rest frame electric field is $\gamma E \hat{x}_2$; and the separator length is foreshortened to L_E/γ , so the electric field is present for time duration L_E/v . This yields rest frame transverse momentum impulse $-eEL_E/v$, which is the same as the laboratory frame transverse momentum impulse.

S-G Deflection in Magnetic Quadrupole

Because their fields vanish on-axis, quadrupoles, either magnetic or electric, erect or skew, provide ideal tests of Stern-Gerlach deflection. Their field boundaries and fields are shown in Fig. 1. Formulas for their field components are given in the figure. Consider a transversely po-

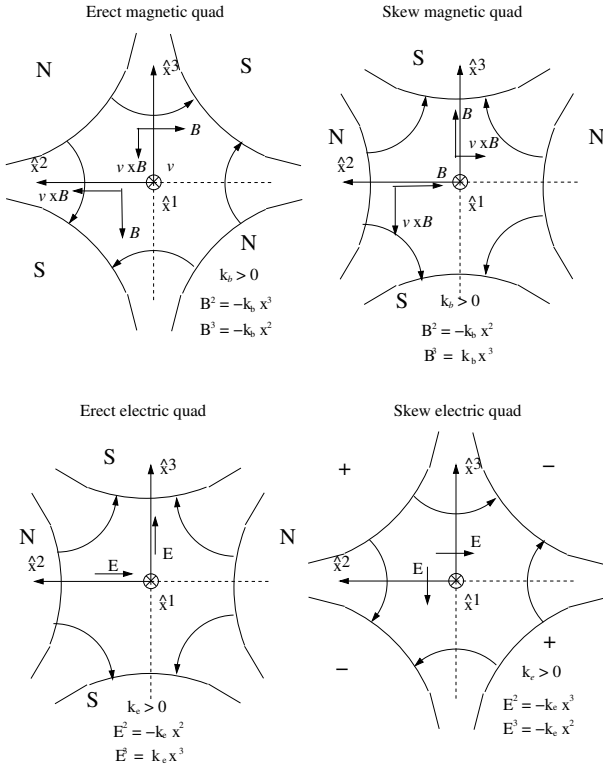


Figure 1: Fields of magnetic and electric quadrupoles, both erect and skew. The hyperbolic curves represent the surfaces of iron poles in the magnetic case, and electrodes in the electric case. In both cases the field lines are normal to these 2D surfaces.

larized electron passing on-axis through such a magnetic quadrupole. The deflection equation is Eq. (26). Can-

celling $(-\gamma)$ from both sides,

$$\begin{pmatrix} -dp_0/dt \\ dp^1/dt \\ dp^2/dt \\ dp^3/dt \end{pmatrix} = \mu_e^* \begin{pmatrix} 0 & 0 & \cdot & \cdot \\ 0 & 0 & 0 & 0 \\ \hat{s}^{*2} B_{,2}^2 + \hat{s}^{*3} B_{,3}^2 & 0 & 0 & 0 \\ \hat{s}^{*2} B_{,2}^3 + \hat{s}^{*3} B_{,3}^3 & 0 & 0 & 0 \end{pmatrix} \begin{pmatrix} 1 \\ v/c \\ 0 \\ 0 \end{pmatrix}. \quad (31)$$

Skew Magnetic Quadrupole. Representing partial derivatives with “ μ ” notation, field components for a *skew* magnetic quadrupole are given by

$$B^2 = -k_b x^2, \quad B^3 = k_b x^3, \quad \text{with } k_b = -B_{,2}^2 = B_{,3}^3. \quad (32)$$

(Reminder: superscripts are indices, not powers.) Because the magnetic field is transverse, there is no coupling to longitudinal spin component \hat{s}^{*1} . The operative equations are

$$\begin{pmatrix} dp^2/dt \\ dp^3/dt \end{pmatrix} = \mu_e^* \begin{pmatrix} -\hat{s}^{*2} k_b & 0 \\ \hat{s}^{*3} k_b & 0 \end{pmatrix} \begin{pmatrix} 1 \\ v/c \end{pmatrix} = \mu_e^* k_b \begin{pmatrix} -\hat{s}^{*2} \\ \hat{s}^{*3} \end{pmatrix}, \quad (33)$$

and the momentum impulses are

$$\Delta p^2 = -\mu_e^* \hat{s}^{*2} k_b \frac{L_q}{v}, \quad \Delta p^3 = \mu_e^* \hat{s}^{*3} k_b \frac{L_q}{v}. \quad (34)$$

Just as the relativistic generalization of electromagnetic deflection was checked in the previous example, the relativistic S-G formulation can be checked by direct Lorentz transformation of the recoil momentum, as calculated in the rest frame. For example, taking $\hat{s}^{*2}=1$, $\hat{s}^{*3}=0$, The $\Delta p^{2'}$ momentum recoil component can be obtained from Eq. (4). Using the transformation properties of B^2 and x^2 , the rest frame S-G force is $\mu_e^* \gamma \partial B^2 / \partial x^2 \hat{x}_2$. Because the quadrupole length is foreshortened to L_q/γ , the interaction duration is L_q/v . Since the recoil is transverse, the laboratory and rest frame momentum recoils are the same;

$$\Delta p^2 = -\mu_e^* k_b \frac{L_q}{v}, \quad (35)$$

in agreement with Eq. (34).

Erect Magnetic Quadrupole Field components for an *erect* magnetic quadrupole are given by

$$B^2 = -k_b x^3, \quad B^3 = -k_b x^2, \quad \text{with } k_b = -B_{,3}^2 = -B_{,2}^3. \quad (36)$$

The operative equations are

$$\begin{pmatrix} dp^2/dt \\ dp^3/dt \end{pmatrix} = \mu_e^* \begin{pmatrix} -\hat{s}^{*3} k_b & 0 \\ -\hat{s}^{*2} k_b & 0 \end{pmatrix} \begin{pmatrix} 1 \\ v/c \end{pmatrix} = \mu_e^* k_b \begin{pmatrix} -\hat{s}^{*3} \\ -\hat{s}^{*2} \end{pmatrix}, \quad (37)$$

and the momentum impulses are

$$\Delta p^2 = -\mu_e^* \hat{s}^{*3} k_b \frac{L_q}{v}, \quad \Delta p^3 = -\mu_e^* \hat{s}^{*2} k_b \frac{L_q}{v}. \quad (38)$$

Realizing that the skew and erect magnets are, in reality, identical, though rotated by 45° , one could have obtained Eqs. (38) by simple rotation of one or the other of the top figures in Figure 1. The formalism is therefore consistent, at least to this extent, for magnetic quadrupoles.

S-G Deflection in Electric Quadrupole

Considering that the calculation can be patterned after the previous examples, for laboratory frame evaluation of the S-G deflection in an electric quadrupole, how can we know whether to use $\mathbb{F}(\mathbf{E}, \cdot)$ from Eq. (7) or $\mathbb{F}(\cdot, \mathbf{B})$ from Eq. (17) as the operative laboratory electromagnetic matrix? Apart from their different predicted recoil directions, especially for $v \ll c$ they give greatly different recoil magnitudes. Even though all components of \mathbf{B} vanish in the laboratory, as already explained, it is $\mathbb{F}(\cdot, \mathbf{B})$ that has the correct inversion symmetry. Again canceling $(-\gamma)$ from both sides, the equations of motion are

$$\begin{pmatrix} -dp_0/dt \\ dp^1/dt \\ dp^2/dt \\ dp^3/dt \end{pmatrix} = \mu_e^* \begin{pmatrix} 0 & 0 & \cdot & \cdot \\ 0 & 0 & \cdot & \cdot \\ 0 & \hat{s}^{*2} E_{,2}^3/c + \hat{s}^{*3} E_{,3}^3/c & 0 & 0 \\ 0 & -\hat{s}^{*2} E_{,2}^2/c - \hat{s}^{*3} E_{,3}^2/c & 0 & 0 \end{pmatrix} \begin{pmatrix} 1 \\ v/c \\ 0 \\ 0 \end{pmatrix}. \quad (39)$$

Erect Electric Quadrupole For an *erect* electric quadrupole the field components are

$$E^2 = -k_e x^2, \quad E^3 = k_e x^3, \quad \text{with } k_e = -E_{,2}^2 = E_{,3}^3. \quad (40)$$

The operative equations are

$$\begin{pmatrix} dp^2/dt \\ dp^3/dt \end{pmatrix} = \mu_e^* \begin{pmatrix} \hat{s}^{*3} E_{,3}^3/c & 0 \\ -\hat{s}^{*2} E_{,2}^2/c & 0 \end{pmatrix} \begin{pmatrix} 1 \\ v/c \end{pmatrix} = \frac{\mu_e^* k_e v}{c^2} \begin{pmatrix} \hat{s}^{*3} \\ \hat{s}^{*2} \end{pmatrix}. \quad (41)$$

Skew Electric Quadrupole For a *skew* electric quadrupole the field components are

$$E^2 = -k_e x^3, \quad E^3 = -k_e x^2, \quad \text{with } k_e = -E_{,3}^2 = -E_{,2}^3. \quad (42)$$

The operative equations are

$$\begin{pmatrix} dp^2/dt \\ dp^3/dt \end{pmatrix} = \mu_e^* \begin{pmatrix} 0 & \hat{s}^{*2} E_{,2}^3/c \\ 0 & -\hat{s}^{*3} E_{,3}^2/c \end{pmatrix} \begin{pmatrix} 1 \\ v/c \end{pmatrix} = \frac{\mu_e^* k_e v}{c^2} \begin{pmatrix} -\hat{s}^{*2} \\ \hat{s}^{*3} \end{pmatrix}. \quad (43)$$

Spin-Orbit Coupling

Spin-Orbit Central Force

Stern-Gerlach deflection plays a significant role in the theory of an atom at rest. This is an example in which

the only laboratory field is purely electric. There is, however, magnetic field in the rest frame of an electron (treated classically) circulating around a point charge. Furthermore, there is non-zero radial electric field on the electron's elliptical or, for simplicity, let us say, circular, orbit.

There are several reasons why the present formalism cannot be applied directly to atomic physics. The most important, of course, is that the analysis has been classical (though relativistic rather than Newtonian). At most the formalism can therefore be applied to "semi-classical atomic theory". But, since the analysis has been stubbornly Newtonian, rather than Hamiltonian, even semi-classical application is not automatic. Furthermore, S-G bending elements have been assumed short enough that the spin direction can be assumed constant during any S-G deflection. This is certainly not valid for an atomic orbit.

In spite of these reservations, it may have mnemonic value, in contemplating modern investigation of relativistic Stern-Gerlach deflection, to pretend to apply the same formalism to atomic orbits treated by classical mechanics. For simplest comparison we will consider a hydrogen atom $Z=1$, in the lowest Bohr model semi-classical case, having $n=1$. We shall treat this system as a tiny storage ring. In this state the (non-relativistic) total energy is given by[9]

$$\mathcal{E}_1 = \frac{m_e e^4}{32\pi^2 \epsilon_0^2 \hbar^2 (1 + m_e/m_p)}. \quad (44)$$

and the orbit radius by

$$a_1 = \frac{4\pi\epsilon_0 \hbar^2}{m_e e^2} = 5.29177 \times 10^{-11} \text{ m}. \quad (45)$$

(In our coordinate convention with indices as superscripts) the particle orbit radius is $r = a_1 - x^2$ where x^2 is a radially-inward displacement, meaning the unit vector \hat{x}_2 always points from the electron toward the nucleus proton. The potential energy, and the radial electric field are

$$V(r) = -\frac{e^2}{4\pi\epsilon_0 r}, \quad (46)$$

$$E^2(r) = -\frac{e}{4\pi\epsilon_0 (a_1 - x^2)^2} = -E_1 \left(1 + \frac{2x^2}{a_1} + \dots \right).$$

where E_1 is positive by definition, and its "1" subscript indicates "first" Bohr orbit. For Stern-Gerlach deflection it is only first derivatives of the field that enter. In this sense the effective electric field components for the inverse square law electric field are

$$\begin{aligned} E^2 &= -2E_1 \frac{x^2}{a_1}, & E_{,2}^2 &= \frac{-2E_1}{a_1}, \\ E^3 &= E_1 \frac{x^3}{a_1}, & E_{,3}^3 &= \frac{E_1}{a_1}. \end{aligned} \quad (47)$$

As in a circular storage ring, in a more or less circular atomic orbit, treated classically, the spin will precess around the normal to the orbit plane, both because of

Thomas and S-G precession (which explicitly violates approximations made up to this point.) Barring possible resonance effects (a possibility we ignore, for now, but will revisit) any effective radial force due to the Stern-Gerlach force acting on spin polarization components lying in the orbit plane will necessarily average to zero. It is true, however, that the spin component normal to the orbit plane, in our notation $\pm \hat{s}^{*3}$, will be conserved in this precession. Any radial force, in our notation F^2 , will be constant, causing the radius of a circular orbit to depend (very weakly) on whether the spin is up or down.

In Figure 1 one notes that the closest match to this field pattern is labeled “erect electric quad”. In this figure, with increasing x^2 the electric field component E^2 varies proportionally with x^2 , and similarly for x^3 and E^3 . Comparing Eqs. (47) with Eqs. (40), one also sees that the linearized Coulomb field components resemble those of an erect electric quadrupole. We can therefore apply Eq. (39), with two of the electric field components set to zero. The operative equations are

$$\begin{pmatrix} dp^2/dt \\ dp^3/dt \end{pmatrix} = \mu_e^* \begin{pmatrix} 0 & \hat{s}^{*3} E_{,3}^3/c \\ 0 & -\hat{s}^{*2} E_{,2}^2/c \end{pmatrix} \begin{pmatrix} 1 \\ v/c \end{pmatrix}. \quad (48)$$

We have already argued that any effect due to \hat{s}^{*2} averages to zero, so we are left with a single equation for the Stern-Gerlach force;

$$F_{\pm}^{SG} = \frac{dp^2}{dt} = \frac{\mu_e^* \hat{s}^{*2} v}{c^2} E_{,3}^3 = \pm \frac{\mu_e^* v}{c^2} \frac{E_1}{a_1}. \quad (49)$$

In the final step, as well as using Eqs. (47), the formula has been simplified to cover just the cases of spin up and spin down. The formula shows that the S-G force simply adds to or subtracts from the Coulomb force, depending on whether the spin is up or down. The ratio of S-G force to Coulomb force is

$$\frac{F_{\pm}^{SG}}{F^{\text{Coul}}} = \pm \frac{\mu_e^*/c}{e} \frac{1}{a_1} \frac{v}{c} = \pm \frac{1/2}{137.0359} \frac{v}{c} = \pm \frac{\alpha^2}{2}. \quad (50)$$

where the intermediate numerical “coincidence” is noted in passing. Of course it cannot be a coincidence at all, since the problem being addressed is the same as the problem Sommerfeld was attacking when he defined his fine structure constant α . It remains, however, to determine whether the magnetic moment value $\mu_B = 5.788382 \times 10^{-5}$ eV/T initially assumed, leads to sensible energy difference between spin-up and spin-down energy levels in our toy semi-classical model.

Spin-Orbit Energy Shift

(Ignoring the reduced mass correction) for electron motion in a circle of radius a_1 at electric field E_1 , the non-relativistic kinetic energy $K_{1,NR}$ and the relativistic momentum $p_1 = m\gamma v$ are given by

$$\begin{aligned} m_e \gamma \frac{v^2}{a_1} &= eE_1, \longrightarrow p_1 c = \frac{eE_1 a_1}{v_1/c} \\ &\longrightarrow K_{1,NR} = eE_1 a_1/2. \end{aligned} \quad (51)$$

Should a next approximation be required for kinetic energy it can be obtained from

$$K_1 = \frac{eE_1 a_1}{2} \left(1 + \frac{3}{2} \frac{eE_1 a_1/2}{m_e c^2} \right). \quad (52)$$

At radius a_1 the potential energy and non-relativistic total energy are

$$V_1 = -\frac{e^2}{4\pi\epsilon_0 a_1}, \quad \mathcal{E}_1 = -\frac{e^2}{8\pi\epsilon_0 a_1}. \quad (53)$$

The only spin-orbit effect encountered so far is equivalent to a change in central force. In the Bohr model, for a given state, the angular momentum quantum condition requires the angular momentum $p_1 a_1$ to be preserved, which requires

$$\frac{\Delta p_1}{p_1} = -\frac{\Delta a_1}{a_1}. \quad (54)$$

For a circular orbit the momentum satisfies $p = \sqrt{2m_e K} = \sqrt{m_e e E_1 a_1}$, which requires

$$\frac{\Delta p_1}{p_1} = \frac{1}{2} \frac{\Delta E_1}{E_1} + \frac{1}{2} \frac{\Delta a_1}{a_1} \quad (55)$$

Combining Eqs.(54) and (55) produces

$$\frac{\Delta a_1}{a_1} = -\frac{1}{3} \frac{\Delta E_1}{E_1}. \quad (56)$$

For circular orbits the total energy \mathcal{E} is half the potential energy $V_1 = e^2/(4\pi\epsilon_0 a_1)$, which varies inversely with a_1 . Combining formulas

$$\frac{\Delta \mathcal{E}_1}{\mathcal{E}_1} = -\frac{\Delta a_1}{a_1} = \frac{1}{3} \frac{\Delta E_1}{E_1} = \frac{1}{3} \frac{F_{\pm}^{SG}}{F^{\text{Coul}}}, \quad (57)$$

where, in the last step, $F_{\pm}^{SG}/F^{\text{Coul}}$ is treated as a fractional change in the central electric field. Substitution from Eq. (50) produces

$$\frac{\Delta \mathcal{E}_1}{|\mathcal{E}_1|} = \frac{1}{3} \frac{F_{\pm}^{SG}}{F^{\text{Coul}}} = \pm \frac{\alpha^2}{6}. \quad (58)$$

As emphasized previously, being classical rather than quantum mechanical, this has just been a toy calculation intended mainly as a “sanity check” of the relativistic formulation. Toward this end, one can compare result (58) with a quantum mechanical calculation of spin-orbit doublet splitting. An exact comparison is impossible because there is not exact correlation between Bohr energy levels and quantum mechanical levels.

A somewhat similar, up-to-date, quantum mechanical spin-orbit doublet separation calculation can be copied from Leighton[9], assuming $Z=1$, $n = 1$, $l = 1$

$$(a) \frac{\Delta \mathcal{E}_1}{|\mathcal{E}_1|} = \frac{\alpha^2}{(2l+1)(l+1)}, \quad \text{for } j = l + 1/2, \quad (59)$$

$$(b) \frac{\Delta \mathcal{E}'_1}{|\mathcal{E}_1|} = \frac{-\alpha^2}{l(2l+1)}, \quad \text{for } j = l - 1/2, \quad l \neq 0. \quad (60)$$

The classical and quantum calculations differ only in the numerical factors, which are $+1/6, -1/6$ in the classical calculation and $+1/6, -1/3$ in the quantum mechanical calculation. This level of agreement more than satisfies the intended sanity check of our relativistic formulation.

Repeating a previous comment, the closeness of a classical to a quantum result should not be surprising; the calculation is more-or-less equivalent to a Sommerfeld calculation that was more-or-less successful in interpreting spectral doublets even before 1920.

What is perhaps surprising, though, is that a crude Newtonian picture of an atom as a tiny storage ring, though wrong, is not flagrantly wrong. Included in this picture is the treatment of the S-G force as a tiny spin-dependent alteration of the central electric force. Niceties such as Thomas precession, and other delicate spin precession effects, are irrelevant in this picture because they simply average to zero without having any influence at all on the stable energy levels. In accelerator physics practice one would be inclined to blame the failure of the classical physics model on incorrect treatment of resonant spin effects. It seems the quantum mechanical Hamiltonian angular momentum addition formalism magically accounts correctly for this behavior.

That an atom can be visualized as a tiny storage ring is just a curiosity. But there is real content to the concept of a storage ring as a giant atom, especially if the beam is polarized and the polarization is “phase-locked”. An atom cannot have very many electrons, but a storage ring can have 10^{10} . Even though these electrons have spreads in position, slope, energy, and spin orientation, there can be enough of them for the polarization to be fed-back and phase-locked to an externally-imposed frequency. With spin precession proportional to magnetic moment, which is known to the precision implied by the values listed in Eq. (1), and all other coordinates phase-locked as well, the storage ring has become a “trap” with parameters stabilized to exquisite precision. Then, much like nuclear magnetic resonance, there is then the possibility of detecting exquisitely small effects superimposed on the centroid motion. Effects too small to be observed over a single revolution can be magnified by the millions, or even billions, of beam revolutions possible in a storage ring.

This concludes the theoretical discussion. Experimental details follow.

PRACTICAL OBSERVATION OF S-G DEFLECTION

A recent conference presentation[10], from a Cornell, Jefferson Lab, University of New Mexico working group, explains how the CEBAF 123 MeV injection line can serve as one big Stern-Gerlach polarimeter measuring the polarization state of the injected electron beam. No physical changes to the line are required and (though not optimal) beam position monitors (BPMs) already present in the line can be used to detect the S-G signals. Most of the remain-

der of this paper is drawn from that report.

The historical Stern-Gerlach apparatus used a uniform magnetic field (to orient the spins) with quadrupole magnetic field superimposed (to deflect opposite spins oppositely) and a neutral, somewhat mono-energetic, unpolarized, neutral atomic beam of spin 1/2 particles. For highly-monochromatic, already-polarized beams produced by Jefferson Lab electron guns, the uniform magnetic field has become superfluous, and every quadrupole in the injection line produces polarization-dependent S-G deflection. The absence of constant magnetic field on the unperturbed electron orbit has the further effect of guaranteeing zero electric field at the electron’s instantaneous position in its own (unperturbed) rest frame. Unlike in the actual Stern-Gerlach configuration, any non-zero electric field in such a frame is proportional to (miniscule) Stern-Gerlach deflections, and can therefore be neglected to good approximation.

Starting from neutral silver atoms, with approximate velocity 500 m/s in the original experiment, for which the angular deflections were roughly $\Delta\theta^{Ag} \approx 0.005$ radians, we can estimate the Stern-Gerlach deflections of 6 MeV electrons in the quadrupoles of a modern-day accelerator. In both cases the transverse force is due to the magnetic moment of a single electron. Magnets in the CEBAF beam line are much like the original (1923) Stern-Gerlach magnets, though the original magnetic field gradient \times length product was several times larger[2] than for typical quadrupoles in the CEBAF injection line¹. But, for simplicity, we compare the deflections of a silver atom and a free electron in identical magnets.

The transverse force is the same irrespective of whether the electron is free or a valence electron in the silver atom. An anticipated deflection of electrons with $\gamma_e = 12$ can be estimated from formulas for the angular deflection, $\Delta p_{\perp}/p_z$, for the ratio of force durations, v^e/v^{Ag} , and for the ratio of longitudinal momenta, p^{Ag}/p^e :

$$\begin{aligned} \frac{\Delta p_{\perp}}{p_z} &= \text{Force} \frac{\text{duration}}{p_z} \\ \frac{v^e}{v^{Ag}} &= \frac{3 \times 10^8}{500} = 6 \times 10^5 \\ \frac{p^{Ag}}{p^e} &= \frac{M^{Ag}}{m_e} \frac{\gamma^{Ag}}{\gamma_e} \frac{v^{Ag}}{v^e} \\ &\approx \frac{108 \times 2000 m_e}{m_e} \frac{1}{12} \frac{500}{3 \times 10^8} \approx 0.03. \end{aligned} \quad (61)$$

In the same magnet we expect 6 MeV electron deflections of order

$$\Delta\theta^{6MeV} \approx 0.005 \times \frac{0.03}{6 \times 10^5} \approx 2.5 \times 10^{-10} \text{ radians.}$$

With drift lengths in the injection line being of order 1 meter, and allowing for the somewhat smaller field integrals, this suggests that the Ångström, which is equal to 10^{-10} m,

¹Some parameters for the original Stern-Gerlach experiment were: central field 0.1 T, peak field gradient 100 T/m, $T = 1350^\circ\text{K}$, magnet length 0.035 m, distance from magnet center to detecting film 0.02 m.

is an appropriate unit for expressing the S-G betatron amplitudes to be expected.

For a dedicated reconfiguration of the beamline optics, the S-G deflection could be enhanced substantially. But, to minimize operational interruption, we first assume no CE-BAF beamline changes whatsoever, so that investigations can be almost entirely parasitic. Because the expected amplitudes are so small, we also consider reducing the beam energy to 6 MeV or less (from 123 MeV) throughout the line, by detuning the intermediate linac section, to increase the S-G effect.

Dual CEBAF electron beam guns produce superimposed 0.25 GHz (bunch separation 4 ns) electron beams for which the polarization states and the bunch phases can be adjusted independently. For example, the (linear) polarizations can be opposite and the bunch arrival times adjusted so that (once superimposed) the bunch spacings are 2 ns and the bunch polarizations alternate between plus and minus. The effect of this beam preparation is to produce a bunch charge repetition frequency of 0.5 GHz different from the bunch polarization frequency of 0.25 GHz. This difference will make it possible to distinguish Stern-Gerlach-induced bunch deflections from spurious charge-induced excitations.

Transverse bunch displacements produce narrow band BPM signals proportional to the f_r Fourier frequency components of transverse beam displacement. Because linac bunches are short there can be significant resonator response at all of the strong low order harmonics of the 0.25 GHz bunch polarization frequency. The proposed S-G responses are centered at odd harmonics, $f_r = 0.25, 0.75, 1.25$ GHz. The absence of beam-induced detector response at these frequencies greatly improves the rejection of spurious “background” bunch displacement correlated with bunch charge. For further background rejection the polarization amplitudes are modulated at a low, sub-KHz frequency which shifts the S-G response to sidebands of the central S-G frequencies.

STERN-GERLACH DEFLECTION OF A RELATIVISTIC PARTICLE

This section is largely repetitive of previous derivations, but from a more elementary, and more practical point of view. It is specialized toward ongoing investigations using a Jefferson lab injection line.

We are primarily interested in the Stern-Gerlach deflection caused by the on-axis passage of a point particle with velocity $v\hat{z}$ and rest frame, transversely-polarized magnetic dipole moment vector $\mu_x^*\hat{x}$, through a DC quadrupole, of length L_q , that is stationary in the laboratory frame K .

It is valid to formulate the calculation with an impulsive approximation, in which the integrated momentum imparted to a particle passing through a quadrupole is small enough to justify neglecting the spatial displacement occurring during the encounter and keeping track of only the

angular deflection.² One also notes the particle speed is conserved because it is only a longitudinal component of force that can change the particle speed. The Stern-Gerlach deflection in the electron’s instantaneous rest frame can simply be copied from well-established non-relativistic formalism[3]; the transverse force is given by

$$F'_x = \mu_x^* \frac{\partial B'_x}{\partial x'}. \quad (62)$$

Following notation of Conte[1], the rest frame magnetic moment is symbolized by μ^* to stress that it is specific to the rest frame, irrespective of whatever reference frame is being discussed. A transverse spin in the laboratory is (by definition) also transverse in the particle rest frame. And, concerning the present calculation, there is no issue of “Lorentz transformation of spins or magnetic moments”, since the S-G deflection is to be calculated in a frame of reference in which the electron remains non-relativistic. In this frame formula (62) has been thoroughly confirmed by experiment.

As viewed in the K' rest frame, the passing magnet is Lorentz-contracted to length $L'_q = L_q/\gamma$, the time spent by the particle in the magnetic field region is L'_q/v , and the integrated, rest frame transverse momentum impulse is

$$\Delta p'_x = F'_x \frac{L'_q}{v} = \frac{\mu_x^*}{v} \frac{\partial}{\partial x'} (B'_x L'_q). \quad (63)$$

To determine B'_x the laboratory magnetic field B_x needs to be Lorentz transformed to the moving frame K' . This produces both an electric and a magnetic field, but it is only the magnetic field that produces Stern-Gerlach acceleration in the particle’s rest frame. The Lorentz transformation yields[4] $B'_x = \gamma B_x$. We conclude that the product $B_x L_q = B'_x L'_q$ is the same in laboratory and rest frames. Since the displacement $x = x'$ and the transverse momentum component $\Delta p_x = \Delta p'_x$ are also invariant for Lorentz transformation along the z axis, Eq. (63) becomes

$$\Delta p_x^{SG} = F_x \frac{L_q}{v} = \frac{\mu_x^*}{v} L_q \frac{\partial B_x}{\partial x}, \quad (64)$$

and similarly for Δp_y^{SG} . The “SG” superscripts have been introduced to distinguish Stern-Gerlach deflections from Lorentz force deflections.

The conclusion so far is that formula (64), derived historically using non-relativistic kinematics, is valid even for relativistic particle speed. Of course, because v cannot exceed c , the transverse force saturates as the particle becomes relativistic. Since the particle momentum continues

²For anomalous electron angular momentum $G = 0.00116$ the spin precession angle occurring during angular deflection $\Delta\theta$ of approximately $G_e \gamma \Delta\theta / (2\pi)$ is negligible. All spins are taken to be purely horizontal (in the x -direction) in both the laboratory and the electron rest frame. Similarly there is no longitudinal magnetic field in either frame.

On-axis in a magnetic quadrupole there is neither magnetic, nor electric field in either the K or the K' frame. Once an electron is displaced by the S-G force, there is non-zero magnetic field in the K frame, and hence non-zero electric field in the K' frame. Solution of the orbit equation with this electric force included is given in the appendix.

to increase proportional to γ , the S-G angular deflection in a fixed excitation quadrupole field falls as $1/\gamma$.

The magnetic field components of an erect DC quadrupole are given by

$$B_x = ky, \quad B_y = kx, \quad \text{where } k = \frac{\partial B_x}{\partial y} = \frac{\partial B_y}{\partial x}. \quad (65)$$

The quadrupole field in the original Stern-Gerlach experiment would, in modern accelerator terminology, be referred to as “skew”. The strong quadrupoles in the CEBAF line under consideration are “erect”.

Treating a quadrupole of length L_q as a thin lens, the Lorentz force on a point particle of mass m and charge e traveling with velocity $v\hat{z}$ through the quadrupole imparts momentum

$$\Delta \mathbf{p} = \mathbf{F}(x, y) \Delta t = eL_q k(y\hat{y} - x\hat{x}). \quad (66)$$

The relativistic longitudinal particle momentum of the particle is $p = \gamma mv$ and its (small, linearized) electromagnetic angular deflections are given by

$$\Delta\theta_x \hat{x} + \Delta\theta_y \hat{y} = \frac{\Delta \mathbf{p}}{p} = q_x x \hat{x} + q_y y \hat{y}, \quad (67)$$

where inverse focal lengths $q_x = 1/f_x$ and $q_y = 1/f_y$ of the quadrupole satisfy

$$q_x = -\frac{eL_q k}{p} = -\frac{L_q c \partial B_y / \partial x}{pc/e} = -q_y. \quad (68)$$

Meanwhile, the Stern-Gerlach deflections are given by

$$\Delta\theta_x^{SG} = \frac{\Delta p_x^{SG}}{p} = \frac{\mu_x^* L_q k}{pv}, \quad (69)$$

and similarly for y . Comparing with Eqs. (68), one sees that the Stern-Gerlach deflection in a quadrupole is strictly proportional to the inverse focal lengths of the quadrupole;

$$\Delta\theta_x^{SG} = -\frac{\mu_x^*}{ec\beta} q_x, \quad \text{and} \quad \Delta\theta_y^{SG} = \frac{\mu_y^*}{ec\beta} q_y, \quad (70)$$

These formulas are boxed to emphasize their universal applicability to all cases of polarized beams passing through quadrupoles. For all practical (electron beam) cases $\beta \approx 1$.

As mentioned previously, the S-G deflection at fixed magnet excitation is proportional to $1/\gamma$. Yet, superficially, deflection formulas (70) show no *explicit* dependence on γ (such as, for example, the denominator factor 12, in Eq. (61)). This is only because the angular deflections are expressed in terms of quadrupole inverse focal lengths. For a given quadrupole at fixed quadrupole excitation, the inverse focal length scales as $1/\gamma$. Expressing the S-G deflection in terms of inverse focal lengths has the effect of “hiding” the $1/\gamma$ Stern-Gerlach deflection dependence, which comes from the beam stiffness.

μ_x^* and μ_y^* differ from the Bohr magneton μ_B only by $\sin \theta$ and $\cos \theta$ factors respectively. Numerically, for

one particular CEBAF quadrupole, Eq. (70) yields Stern-Gerlach-induced, Courant-Snyder betatron amplitude proportional to

$$\sqrt{\beta_x} \Delta\theta_x^{SG} = -(1.93 \times 10^{-13} \text{ m}) \sqrt{\beta_x} q_x, \quad (71)$$

and similarly for y . The $\sqrt{\beta}$ factor has been included because the transverse displacement Δx_j at downstream location “j” caused by angular displacement $\Delta\theta_i$ at upstream location “i” is given (in either plane) by

$$\Delta_j = \sqrt{\beta_j \beta_i} q_i \sin(\psi_j - \psi_i). \quad (72)$$

where $\psi_j - \psi_i$ is the betatron phase advance from “i” to “j”, and Δ_j stands for either Δx_j or Δy_j .

S-G SPECIFIC BEAM PREPARATION

The smallness of the S-G signal, especially relative to unintentional charge-sensitive cavity responses, makes it critical for the polarized beam to be prepared for maximum rejection of spurious background.

Recent ILC-motivated BPM performance investigations [11][12] are relevant to our proposed Stern-Gerlach (S-G) detection experiment. Resonant beam position detection relies on two TM cavities. The charge-sensitive cavity (needed to normalize the charge) is tuned to resonate in a transversely symmetric mode at the bunch frequency. The position-sensitive cavity is tuned to resonate in a transversely anti-symmetric mode at the same bunch frequency.

(By the Heisenberg uncertainty principle) it would not be feasible to locate a single mono-energetic electron with usefully small transverse accuracy. This makes the electron charge e unnaturally small for present purposes. For comparison we define a “standard macro-charge” as the charge of $N_e = 10^{10}$ electrons, which is a typical number of electrons in each bunch in an ILC BPM prototype test, for example at the KEK Accelerator Test Facility (ATF). Classical (rather than quantum) mechanics is adequate for treating the centroid motion of such a large number of electrons, even as regards their mean spin orientation.

A CEBAF beam is CW, with beam current of, say, $160 \mu\text{A}$, which corresponds to a current of about 10^5 (just-defined) macro-charges per second. For S-G detection the Ångstrom is a convenient transverse length unit for S-G detection. For comparison, successful ILC operation the transverse beam positions need to be controlled to about $\pm 10 \text{ Å}$.

The bunch structures of the CEBAF injector (123 MeV, $160 \mu\text{A}$, 0.5 GHz) and ATF (1.3 GeV, $N_e e = 10^{10} e$ macro-charge at 5 Hz pulse rate) are very different. We ignore the energy difference, which is thought to be unimportant for the comparison. For a typical cavity resonator quality factor of $Q_r = 10^4$ and frequency of 1 GHz, the cavity discharging time is far shorter than the ATF repetition period. This makes it appropriate to treat the ATF resonant response on a pulse-by-pulse basis. Essentially different in

time structure, the CEBAF resonator response is continuous wave (CW) with the previously-defined macro-charges passing through the cavity at 100 kHz rate.

In a linac beam line, the fact that each bunch passes an S-G sensitive BPM only once, makes it hard to arrange for the polarization of successive bunches to be different. But, as already explained, high frequency bunch polarization modulation frequency is made possible by superposing staggered bunch trains having different polarizations. Figure 2 illustrates our planned, superimposed CEBAF bunch train. Bunches are labeled A in one of two pre-superimposed bunch trains and B in the other. Time domain plots are on the left, frequency spectra on the right. The foreground S-G betatron signal oscillates at (harmonics of) 0.25 GHz, while the background charge signal oscillates at (harmonics of) 0.5 GHz. For resonant cavity BPMs the S-G detector would be tuned to a harmonic of the 0.25 GHz fundamental, for example to the third or fifth harmonic, for more convenient (smaller) cavity dimensions.

We assume the polarization of the superimposed A and B beams are also modulated with (low) frequency ω_m . The time domain, $ip(t)$ current-polarization products of the separate A and B beams are then given by

$$ip^A(t) = \sum_{n=-\infty}^{\infty} \delta(t - nT_0)(A + a \cos \omega_m t) \quad (73)$$

$$ip^B(t) = \sum_{n=-\infty}^{\infty} \delta(t - T_0/2 - nT_0)(A - a \cos \omega_m t).$$

and are plotted on the left in Figure 2. The modulation amplitude a is drawn much smaller in magnitude than the unmodulated polarization amplitude A . But over-modulation, with values of a as great as $2A$, to maximize the side-band amplitudes, might be practical. There are two essential differences between the A and B beams. The beam pulses are shifted in time by one half cycle and the sign of the modulation is reversed. The modulation frequency ω_m , for which the frequency is expected to be about 1 kHz, is exaggerated by many orders of magnitude in this figure, since $f_0 = 1/T_0$ is about 0.75 GHz. Champeney[14] gives the A-beam, cosine-modulated current-polarization Fourier transform $IP^A(\omega)$ to be

$$IP^A(\omega) = \sum_{n=-\infty}^{\infty} \frac{2\pi}{T_0} \left(A \delta\left(\omega - n \frac{2\pi}{T_0}\right) + \frac{a}{2} \delta\left(\omega - n \frac{2\pi}{T_0} + \omega_m\right) + \frac{a}{2} \delta\left(\omega - n \frac{2\pi}{T_0} - \omega_m\right) \right). \quad (74)$$

The Fourier transform of the B-beam, sine-modulated, current-polarization Fourier transform is obtained by multiplying by the time-shift factor, $e^{-iT_0\omega/2}$ for which, when it is moved inside the summation, its ω factor can be replaced by $2\pi n/T_0$, due to the delta function having argument $\omega - 2\pi n/T_0$. The resulting $(-1)^n$ factor causes the sign alternation exhibited in the middle right graph in Figure 2. Because the modulation frequency is so low the cor-

responding time shift of the modulation is being neglected.

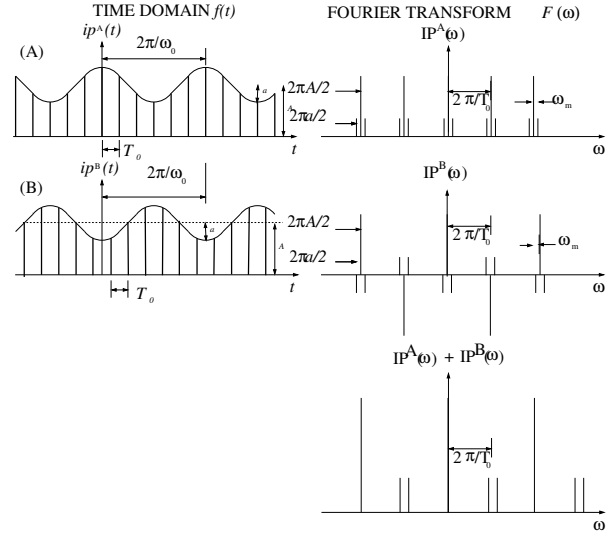


Figure 2: Time domain and frequency domain beam pulses for the A and B staggered, modulated-polarization beams. It is current-weighted polarization spectra that are plotted in these figures. The current spectra themselves are obtained by suppressing the modulation sidebands. In the A+B spectra the odd harmonics of beam current cancel, effectively doubling the fundamental current frequency from 0.25 GHz to 0.5 GHz. But the current-weighted polarization side bands survive as odd harmonics of 0.25 GHz.

SIGNAL LEVELS AND BACKGROUND REJECTION

According to Eqs. (70) the transverse displacement magnitude Δ at distance L downstream of a quadrupole of strength q is given by

$$\Delta = (1.932 \times 10^{-13} \text{ m}) q L \quad (75)$$

$$\approx (2 \times 10^{-13} \text{ m}) \times 1/\text{m} \times 10\text{m} = 0.02 \times 10^{-12} \text{ m}.$$

The installed CEBAF beam position monitors are “antenna BPM’s”, each consisting of four short (approximately 4 cm long), longitudinal, probe antennas, symmetrically-located azimuthally, within cylindrical beam tubes. Not themselves being narrow band, these BPMs are more noise-sensitive than resonant BPMs. But they have the important advantage of responding to both symmetric and anti-symmetric modes over large frequency range, for example at both 0.75 GHz and 1.0 GHz, with the responses easily separable by narrow band external spectral analysis.

Barry[15] gives the transverse impedance of standard CEBAF BPMs to be $Z_{\perp} = 3800 \text{ V/m}$. Taking $200 \mu\text{A}$ as a satisfactory beam current, the corresponding BPM power

level would be

$$\begin{aligned} P &\approx (0.0002)^2 \times 3800 \times (0.02 \times 10^{-10}) \\ &= 3.0 \times 10^{-16} \text{ W} = -125 \text{ dBm}. \end{aligned} \quad (76)$$

At room temperature the thermal noise in a 1 Hz bandwidth is given by

$$\begin{aligned} P_{\text{noise}} &= kT\Delta f = (1.38 \times 10^{-23} \text{ J/K}) \times (293 \text{ K} \times 1 \text{ Hz}) \\ &= 4.1 \times 10^{-21} \text{ W} = -174 \text{ dBm} \end{aligned} \quad (77)$$

This calculation suggests that, with seconds-long data collection, the S-G signal level will be large enough to be distinguishable from thermal noise. (A much lower thermal noise floor could be achieved with cryogenic detection.)

A more serious impediment to S-G detection is spurious cavity response to bunch charge rather than to bunch polarization. We now review the procedures to be employed in distinguishing S-G signals from background.

Centered cavity. Conventional BPM beam centering relies on exact cavity centering for which, ideally, there is no direct charge excitation of the position sensitive cavity. Roughly speaking, the previously-described ILC BPM prototypes have so far achieved absolute transverse position reproducibility of $\pm 15 \text{ nm}$, for bunch to bunch variation of beam bunches containing $N_e = 10^{10}$ electrons. This is roughly an order of magnitude greater than (i.e. inferior to) their theoretical-minimum expected resolution of $\pm 1.8 \text{ nm}$. The authors (persuasively) ascribe their BPM performance short-fall primarily to error sources other than thermal noise, such as instrument imperfections or cross-talk from spurious, mode-forbidden response to bunch charge.

The “good news” to be drawn from the ILC $\pm 1.8 \text{ nm}$ noise floor is that, with long time averaging, because of the high average CEBAF beam current, coherent betatron oscillation amplitudes as small as, say, 0.02 \AA , can be expected to emerge from thermal noise, even with room temperature detectors. The “bad news” is that there is little reason to suppose that cavity-centering S-G selectivity (relative to spurious background excitation) can be improved appreciably by increasing data collection times. Based on this estimate, an S-G induced betatron amplitude of 0.02 \AA , though distinguishable from thermal noise in a single, carefully-centered, conventional resonant BPM, can be expected to be dwarfed by a background/foreground ratio of more than one thousand. This limitation is specific to the beam position and beam charge signals occurring at the same frequency, as in conventional beam position centering.

Based in this discuaaion, accuracies as small as $\pm 20 \text{ \AA}$ should be achievable with centered transverse resonant BPMs. We are striving to measure betatron amplitudes 1000 times smaller. Mainly we need to make the case that rejection of spurious BPM signals caused by the beam charge (rather than the beam polarization) can be improved by three orders of magnitude compared to their influence on currently achievable transverse resonant BPM accuracy.

The further selectivity improvement factors to be expected are surveyed next.

Disjoint polarization and charge frequencies. As explained earlier, the polarized beam will be tailored so that the bunch polarization and bunch charge frequencies are different. In this condition the BPM cavity is sensitive to polarization at one frequency (0.75 GHz) and to charge at a different frequency (such as 0.5, or 1.0 GHz). Ideally, the resulting frequency domain filtering will suppress the spurious background response by many orders of magnitude. More realistically, there will still be background response, for example due to the small Fourier component of charge excitation due to not-quite-cancelling beam A and beam B currents.

Empirical beam steering to null “common mode” BPM responses at both even and odd harmonics of 0.25 MHz (which would all vanish for ideal beam preparation) is especially useful for rejecting spurious background excitation. This cancels both off-axis background excitation at the fundamental beam charge frequency and charge-imbalance background “leakage” from even harmonics to odd harmonics, while preserving the foreground S-G response differentially in the odd harmonics.

One can expect significant background/foreground suppression from these common mode suppression and differential mode frequency domain filtering measures—perhaps three orders of magnitude.

Sideband shift of polarization frequency. As explained previously, the effect of low frequency modulation of the beam polarizations is to shift the S-G response to sidebands of the central cavity resonance. To the extent the beam currents are unaffected by this modulation, the sideband response will provide a pure S-G signal. In practice the beam currents will, in fact, also be weakly modulated which will allow some background signal to leak out to the side-band frequencies. Still one can expect significant background/foreground suppression—perhaps two orders of magnitude.

Multi-detector response modeling. In the CEBAF line under discussion the foreground S-G response will be monitored, with various (well known) degrees of sensitivity, in both x and y planes, at 19 BPM locations. The extent to which the beam charges are (unintentionally) being low-frequency modulated at the gun can be parameterized with a few parameters, say 4, the main one describing charge imbalance. Modulation of initial (low energy) beam angles will also mimic S-G signals in individual BPMs. The corresponding betatron amplitudes are adiabatically damped by the subsequent acceleration, but they may remain significant. But there is no reason to suppose that the downstream sensitivity to starting beam conditions is correlated with S-G sensitivity. If true, any spurious side-band responses can be subtracted by a model fitted to match the total responses at all BPMs. Perhaps two orders of magnitude selectivity improvement can be achieved.

Lock-in signal detection. Though not mentioned previously, it is also true that the resonator responses will be

coherent with the beam bunch frequency. By lock-in detection, the in-phase and out-of-phase S-G sideband deflections can be determined individually. As well as improving noise rejection, this can serve to corroborate the response model just described. Perhaps one more order of magnitude selectivity improvement can be achieved.

Multiplied together, the possibility of achieving eight orders of magnitude rejection of spurious background has been described. This seems conservatively greater than the required three orders of magnitude indicated earlier. Another factor of 6 improvement might be achieved by lowering the beam energy entering the transfer line from 6 MeV to 1 MeV. This would be satisfactory for an initial proof of principle, but would not be tolerable for eventual routine polarimetry during production CEBAF running.

RECAPITULATION AND ACKNOWLEDGEMENTS

The intended purpose for this paper has been to provide technical back-up for an experimental program confirming our understanding of Stern-Gerlach deflection. Apart from the fundamental physical significance of Stern-Gerlach physics, the use of the S-G effect for non-destructive, high analysing power, relativistic electron polarimetry, is an essential next step in the gradual improvement of spin control in storage rings. Such polarimetry will be obligatory for any storage ring determination of the electric dipole moment of the electron.

Discussion in this paper of practical S-G detection has been limited to linac electron beams, because this is the only equipment that is immediately available without substantial development effort. The eventual application of Stern-Gerlach deflection for beam polarimetry is needed far more for polarization control in storage rings, especially for “frozen spin” operation. In a linac a single electron passes a single BPM only once; in a storage ring each electron passes through the same BPM millions of times per second. This greatly favors a storage ring over a linac for S-G detection. With proper phase control, in frozen spin, or pseudo-frozen spin storage ring operation, the repetitive passage through the same high-Q cavity can, in principle, increase the S-G response by another huge factor. Furthermore the beam current in storage ring, even with polarized beam, can be far higher in a storage ring than in a linac. These considerations make Stern-Gerlach polarimetry in a storage ring very promising.

As mentioned previously, the experimental methods described in the previous section have been developed by a working group made up of the authors of reference [10]. These ideas depend on experience gained during the design and implementation of polarized electron beams for the CEBAF accelerator at Jefferson Lab. Credit for the most important idea of all (toggling polarization) which is expected to make S-G detection possible, belongs to the Jefferson lab injection group. This capability depends critically on polarized beam preparation tools developed for

the Jefferson lab physics program.

I would like to acknowledge the numerous conversations I have had on this theoretical aspects of this subject with Saul Teukolsky and Eanna Flanagan. As already explained, experimental aspects have been developed in collaboration with Joe Grames, Reza Kazimi, Matt Poelker, Riad Suleiman, and Brock Roberts.

APPENDIX

S-G deflection of an electron passing on-axis through a quadrupole has been calculated approximately in the body of the paper. For purposes of planning experimental corroboration of the formulas this degree of accuracy is sufficient. Deviations from the simple calculation are considered in this appendix. The magnetic and electric fields in the electron rest frame are

$$\mathbf{B}' = \gamma k(y'\hat{\mathbf{x}} + x'\hat{\mathbf{y}}), \quad \mathbf{E}' = \gamma\beta ck(-x'\hat{\mathbf{x}} + y'\hat{\mathbf{y}}). \quad (78)$$

For a vertically polarized electron the only rest frame magnetic moment is μ_y^* , the only non-zero S-G force is horizontal

$$F^{SG'}_x = \frac{\partial(\boldsymbol{\mu} \cdot \mathbf{B})}{\partial x'} = \mu_y^* \frac{\partial B'_y}{\partial x'} = \mu_y^* \gamma k, \quad (79)$$

and, for an on-axis particle, this is the only force. To lowest approximation the motion in the rest frame is purely horizontal. To next approximation, as x deviates from zero, there is electromagnetic force

$$F^{EM'}_x = -eE'_x - e\beta c \frac{dx'}{dt'} \hat{\mathbf{x}} \times B'_y \hat{\mathbf{y}} \Big|_x = e\gamma\beta ckx'. \quad (80)$$

The horizontal equation of motion is

$$\frac{d^2 F'}{dt'^2} = \frac{e\gamma\beta ck}{m_e} \left(x' + \frac{\mu_x^*}{e\beta c} \right) \equiv \omega'^2 \tilde{x}', \quad (81)$$

where $\tilde{x}' = x' + \mu_x^*/(e\beta c)$. Matching initial conditions, the solution, in ascending powers of μ_x^* , is

$$\tilde{x}' = \frac{\mu_x^*}{e\beta c} \cosh \omega' t' = \frac{\mu_x^*}{e\beta c} \left(1 + \frac{(\omega' t')^2}{2} + \dots \right). \quad (82)$$

Using $x' = x$, after rest frame time duration $t' = (L_q/\gamma)/v$, the exit laboratory particle displacements and slopes are

$$x_{\text{exit}} = \frac{\mu_x^* k L_q^2}{2m_e \gamma v^2}, \quad \Delta\theta^{SG} \approx \frac{\mu_x^* k L_q}{m_e \gamma v^2}. \quad (83)$$

This agrees with Eq. (69).

REFERENCES

- [1] M. Conte, et al., *The Stern-Gerlach interaction between a traveling particle and a time varying magnetic field*, arXiv:physics/0003069v1 [physics.acc-ph], 2000
- [2] B. Friedrich and D. Herschbach, *Space Quantization: Otto Stern's Lucky Star*, Daedalus, Vol. 127, No. 1, pp. 165-191, 1998

- [3] J. Porter, R. Pettifer, and D. Leadly, *Direct demonstration of the transverse Stern-Gerlach effect*, American Journal of Physics, **71**, 1103, 2003
- [4] J. Jackson, *Classical Electrodynamics*, 3rd edition, John Wiley, 1998
- [5] N. Mott and H. Massey, *The Theory of Atomic Collisions*, third edition, Oxford University Press,
- [6] A. Steane, *Relativity Made Relatively Easy*, Oxford University Press, 2012
- [7] R. Hagedorn, *Relativistic Kinematics*, W.A. Benjamin 1963
- [8] R. Fitzpatrick, *Maxwell Equations and ...*, Infinity Science Press, 2008
- [9] R. Leighton, *Principles of Modern Physics*, McGraw Hill, 1959
- [10] R. Talman, J. Grames, R. Kazimi, M. Poelker, R. Suleiman, and B. Roberts, *The CEBAF Injection Line as Stern-Gerlach Polarimeter*, Spin-2016 Conference Proceedings, in preparation, 2016
- [11] Y. Inoue, et al., *Development of a high-resolution cavity-beam position monitor*, PRST-AB **11**, 062801, 2008
- [12] S. Walston, et al., *Performance of a high resolution cavity beam position monitor system*, Nuclear Instruments and Methods in Physics Research A, 578, p1, 2008
- [13] Siwon Jang et al., *Development of a cavity-type beam position monitor with high resolution for ATF2*, Proceedings of IPAC2013, Shanghai, China, 2013
- [14] D.C. Champeney, *Fourier Transforms and Their Physical Applications*, Academic Press, 1973
- [15] W. Barry, *A General Analysis of Thin Wire Pickups for High Frequency Beam Position Monitors*, CEBAF PR-90-024, 1990